Interplay between superconductivity and flux phase in the t-J model

E. Cappelluti and R. Zeyher
Max-Planck-Institut für Festkörperforschung, Heisenbergstrasse 1, D-70569 Stuttgart, Germany
(Received 3 June 1998)

We study the phase diagram of the t-J model using a mean field type approximation within the Baym-Kadanoff perturbation expansion for Hubbard X operators. The line separating the normal state from a d-wave flux or bond-order state starts near optimal doping at $T=0$ and rises quickly with decreasing doping. The transition temperature T_c for d-wave superconductivity increases monotonically in the overdoped region towards optimal doping. Near optimal doping a strong competition between the two d-wave order parameters sets in leading to a strong suppression of T_c in the underdoped region. Treating for simplicity the flux phase as commensurate the superconducting and flux phases coexist in the underdoped region below T_c, whereas a pure flux phase exists above T_c with a pseudogap of d-wave symmetry in the excitation spectrum. We also find that incommensurate charge-density-wave ground states due to Coulomb interactions do not modify strongly the above phase diagram near the superconducting phase, at least, as long as the latter exists at all. [S0163-1829(99)01609-4]

I. INTRODUCTION

It is widely accepted that the mechanism causing high-T_c superconductivity in the cuprates is intimately related to the underlying properties of the normal state. However, there exists presently no agreement on what an appropriate and correct description of the normal state is. One reason for this is that experiments indicate the presence of a whole variety of important fluctuations in the normal state. At low dopings antiferromagnetic fluctuations dominate.[1,2] The associated quantum critical point, however, lies far apart from optimal doping so that the relevance of magnetic fluctuations for high-T_c superconductivity is not evident. Other fluctuations which have been considered to be relevant in the normal state are associated with resonance-valence bonds,[3–6] flux phases,[7–9] stripes,[10,11] or charge density waves.[12,13] The close proximity of high-T_c superconductivity and structural phases or crossovers also follows from the experimental observation of a spingap or pseudogap of d-wave symmetry in the underdoped regime of the cuprates.[14–18] It is thus desirable to study in more detail the phase diagram of models relevant to the cuprates and to identify instabilities, their symmetries and their interactions.

The low-energy physics of the CuO_2 layers of the cuprates is well described by the t-J model.[3,19] In order to be able to carry out systematic approximations the two spin degrees of freedom per site are often increased to N degrees of freedom so that $1/N$ can be used as a small parameter.[20,21] For our purposes it is convenient to consider two spin degrees of freedom as in the original model and to extend the number of orbitals per site from one to $N/2$. In this way the symmetry group of the Hamiltonian of the t-J model is enlarged from SU(2) to the symplectic group Sp($N/2$). Based on $1/N$ expansions it has been shown that this model possesses at large N's two intrinsic instabilities.[22] The first one[23–25] is associated with d-wave superconductivity and is obtained in $O(1/N)$. The second one[25–28] is related to a flux or bond-order wave state of d-wave symmetry and is obtained already in the leading order $O(1)$. The instability towards superconductivity is found for all dopings; the corresponding transition temperature T_c increases from the overdoped side with decreasing doping. Near and below optimal doping the second instability sets in. It occurs in the d-wave channel for the relevant region of parameters. Both its location and its symmetry fits well to the experimental observations of a d-wave pseudogap in the underdoped region. It is thus of much interest to study these two intrinsic instabilities of the t-J model in more detail and this is the subject of this paper.

One obstacle for such a study is the fact that the two instabilities occur in different orders of the $1/N$ expansion. Whereas the transition between the normal and charge-density wave or flux states can be obtained by comparing $O(1)$ contributions to the free energy the superconducting part is of $O(1/N)$. Nevertheless, the calculation of the superconducting phase boundary is unique and involves only Green's functions of leading order in the $1/N$ expansion. The position of the boundary in the phase diagram, on the other hand, depends on the value of N. We will use the $1/N$ expansion in the sense that it allows to select a set of diagrams which are the leading ones at least at large N's. After this selection has been made we put $N=2$. The anomalous self-energy of $O(1/N)$ contains quite a number of terms. It has recently been shown that only the d-wave contributions are important and that for this symmetry the retarded terms cancel each other to a large extent. To simplify our treatment we will thus only keep instantaneous terms in the d-wave channel for the superconducting part.

In the following we will enforce the constraints of the t-J model by using X operators.[21,29,30] Such a formulation is not more involved than the more familiar one using a slave boson formulation. It has, however, the advantage that all quantities such as the order parameters are gauge invariant in the sense of slave boson theory. The outline of the paper is the following. In Sec. II the formalism of our approach is introduced and in Sec. III we discuss the instability of the normal state towards incommensurate and commensurate flux phases, clarifying the range of validity of treatments which only take commensurate flux phases into account. The inter-

play between superconductivity and flux phase is discussed in detail in Sec. IV. Finally we investigate in Sec. V the role of phase separation and the effect of Coulomb interaction on the phase diagram.

II. MEAN-FIELD EQUATIONS IN TERMS OF X OPERATORS

Using X operators the Hamiltonian of our generalized t-J model has the form

$$H=-\sum_{\substack{ij\\p=1\cdots N}}\frac{t_{ij}}{N}X_i^{p0}X_j^{0p}+\sum_{\substack{ij\\p,q=1\cdots N}}\frac{J_{ij}}{4N}X_i^{pq}X_j^{qp}-\sum_{\substack{ij\\p,q=1\cdots N}}\frac{J_{ij}}{4N}X_i^{pp}X_j^{qq}+\sum_{\substack{ij\\p,q=1\cdots N}}\frac{V_{ij}}{2N}X_i^{pp}X_j^{qq}. \quad (1)$$

i and j run over the sites of a lattice. For $N=2$ the operators X_i^{pq} are identical with the projection operators $|_i^p\rangle\langle_i^q|$, where $|_i^p\rangle$ denotes for $p=0$ the empty state and for $p=1,2$ singly occupied states at site i with spin up and down. t_{ij} and J_{ij} are hopping and exchange constants, respectively, and both are assumed to act only between nearest neighbors. The last term in Eq. (1) describes the Coulomb repulsion between electrons.

The extension from $N=2$ degrees of freedom per site to a general N is accomplished by introducing a flavor index $\mu=1,\ldots,N/2$ which enumerates $N/2$ copies of the original orbital. The index p is then a composite index $p=(\sigma,\mu)$, where σ denotes a spin index, and can be chosen to run from 0 to N. The X operators are in general no longer projection operators but are assumed to obey still the commutation rules

$$[X_i^{pq},X_j^{rs}]_{\pm}=\delta_{ij}(\delta_{qr}X_i^{ps}\pm\delta_{sp}X_i^{rq}). \quad (2)$$

The upper (lower) signs in Eq. (2) hold for fermionlike (bosonlike or of mixed nature) X operators. Per definition, fermionlike operators have the internal indices $p=0,q>0$ or $q=0,p>0$, bosonlike ones $p=q=0$ or $p,q>0$. Moreover, the diagonal X operators are assumed to obey the constraint

$$X_i^{00}+\sum_{p=1\cdots N}X_i^{pp}=\frac{N}{2}. \quad (3)$$

In the usual case $N=2$ both Eqs. (2) and (3) are fulfilled, and Eq. (3) is just the completeness relation. For a general N Eq. (3) means that at most $N/2$ electrons can occupy the N states at site i since X_i^{00} is a non-negative operator.[30] Moreover, it can be shown that the problem is completely specified if one assumes, in addition, that the diagonal operators X_i^{pp} are projection operators for $p>0$, exactly as in the case $N=2$.[30] Before proceeding we want to introduce the notation we will use in the following. The index 1 in $X(1)$ denotes all the degrees of freedom (internal indices p_1,q_1, imaginary time τ_1, site index i_1) of the X operator, so that

$$1=\left(\begin{array}{c}p_1q_1\\ \overline{1}\end{array}\right),$$

where $\overline{1}$ stands for $\overline{1}=(i_1,\tau_1)$.

Following the Baym-Kadanoff formalism,[31,21,29] we define the single particle nonequilibrium Green's function in the presence of an external source K by

$$G(12)=-\langle TSX(1)X(2)\rangle/\langle S\rangle, \quad (4)$$

$$S=T\exp\left[\int d1K(1)X(1)\right]. \quad (5)$$

In Eqs. (4) and (5) T is the time ordering operator and K^{pq} the external source which is assumed to couple only to bosonlike operators X^{pq}. $\int d1$ means $\Sigma_{p_1,q_1,i_1}\int_0^\beta d\tau_1$ where β is the inverse temperature. It is convenient to introduce a normalized Green's function g such that Dyson's equation has the usual delta function on the right side[29,32]

$$\int d2[G_0^{-1}(12)-\Sigma(12)]g(21')=\delta(1-1'), \quad (6)$$

where G_0 is given by

$$G_0^{-1}(12)=\delta(1-2)\frac{\partial}{\partial\tau_2}-\delta(\overline{1}-\overline{2})[K^{00}(\overline{1})\delta_{q_1q_2}-K^{q_1q_2}(\overline{1})] \quad (7)$$

and

$$\Sigma(12)=-\int d3v(132)\langle X(3)\rangle+\int d3d4d5v(134)g(45)\gamma(52;3). \quad (8)$$

The explicit expression for the function v is

$$\begin{aligned}v(123)=\delta(\tau_2-\tau_1)\delta(\tau_3-\tau_1)\{&(t_{i_1i_3}+J_{i_1i_2}/2\delta_{i_1i_3})\\&\times[\delta_{q_10}\delta_{q_20}(1-\delta_{p_30})\delta_{p_2p_1}\delta_{q_2p_3}\\&-\delta_{p_10}\delta_{p_30}(1-\delta_{q_30})\delta_{p_2q_3}\delta_{q_1q_1}]\\&+[t_{i_1i_3}+(J_{i_1i_2}/2-V_{i_1i_2})\delta_{i_1i_3}]\\&\times[\delta_{q_10}\delta_{q_30}(1-\delta_{p_30})\delta_{p_20}\delta_{q_2q_1}\delta_{p_3p_1}\\&-\delta_{p_10}\delta_{p_30}(1-\delta_{q_30})\delta_{p_2p_1}\delta_{q_20}\delta_{q_3q_1}]\}.\end{aligned} \quad (9)$$

The square bracket on the right-hand side of Eq. (9) contains two contributions: The first one describes the hopping of a hole between nearest neighbors with a spin-flip, the second one without a spin-flip.

The mean field approximation is usually defined as an approximation for the self-energy Σ in which Σ contains all skeleton diagrams which are at most linear in g. This means in our case that the vertex γ should be approximated by the contribution of zeroth order in g.[33] Such an approximation, however, would violate Luttinger's theorem for every N. Moreover, the relation between the number of particles at a site and the chemical potential would be not unique and depend on the way one calculates it. One way to get rid of these artifacts is to keep in the normal part of Σ only those terms which also are present in the large-N limit and then to put $N=2$. Another justification for such a procedure is the following: The leading normal and anomalous parts of Σ in Eq.

(8) are of $O(1)$ and $O(1/N)$, respectively, in the $1/N$ expansion. The calculation of the superconducting transition temperature involves in leading order only normal self-energies of $O(1)$, which, however, may already describe modulated phases. Calculations based on $1/N$ expansions thus suggest that first one should solve the $O(1)$ normal state problem in leading order of the $1/N$ expansion which may already imply the consideration of modulated phases. In a second step the solution is then used to solve the superconducting part in leading order in $1/N$. It has been found that the mean-field expression for the anomalous Σ is in general quite a good approximation for the total $O(1/N)$ contribution to the anomalous self-energy. Taking this for granted one arrives exactly at the above procedure to calculate Σ.

Before working out the details of the above approximation for Σ it is useful to summarize the $O(1)$ results for Σ and g in the normal, unmodulated phase. In leading order of the $1/N$ expansion the vertex γ in the self-energy can be approximated by the bare one, i.e., by

$$\gamma(12;3)=\delta(\overline{1}-\overline{2})\,\delta(\overline{2}-\overline{3}) \times[\,\delta_{p_1 0}\delta_{p_2 0}\delta_{p_3 q_1}\delta_{q_3 q_2}-\delta_{q_1 0}\delta_{q_2 0}\delta_{q_3 p_1}\delta_{p_3 p_2}]. \tag{10}$$

Also in leading order of the $1/N$ expansion the expectation value of bosonic operators can be calculated in the absence of source field via

$$\langle X^{pq}(\overline{1})\rangle=\delta_{pq}g\begin{pmatrix}0q & q0\\ \overline{1} & \overline{1^+}\end{pmatrix}. \tag{11}$$

Inserting Eq. (10) into Eq. (8) the self-energy is frequency independent for zero source fields. Denoting it after a Fourier transform by $\epsilon(\mathbf{k})$ we obtain for g

$$g(\mathbf{k},i\omega_n)=\frac{1}{i\omega_n-\epsilon(\mathbf{k})-\lambda+\mu}, \tag{12}$$

with

$$\epsilon(\mathbf{k})=\delta\epsilon_0(\mathbf{k})+\alpha(\mathbf{k}). \tag{13}$$

$\epsilon_0(\mathbf{k})$ is the free electron dispersion $\epsilon_0(\mathbf{k})=-t(\mathbf{k})/2$, and the doping δ, the function α, and the shift λ are determined by the following expressions:

$$n=1-\delta=\frac{2}{N_c}\sum_{\mathbf{p}} f\left[\frac{\epsilon(\mathbf{p})+\lambda-\mu}{T}\right], \tag{14}$$

$$\lambda=\frac{1}{N_c}\sum_{\mathbf{p}} t(\mathbf{p})\,\eta(\mathbf{p})-\frac{1}{2}\left[\frac{J(0)}{2}-V(\mathbf{q}\to 0)\right]n, \tag{15}$$

$$\alpha(\mathbf{k})=-\frac{1}{2N_c}\sum_{\mathbf{p}} J(\mathbf{k}+\mathbf{p})\,\eta(\mathbf{p}). \tag{16}$$

N_c is the total number of sites, $f(x)$ the Fermi function $f(x)=1/[\exp(x)+1]$, and $\eta(\mathbf{k})=f[(\epsilon(\mathbf{k})+\lambda-\mu)/T]$. $J(\mathbf{q})$ is defined by $J(\mathbf{q})=2J[\cos(q_x)+\cos(q_y)]$, where J is the coupling constant J_{ij} for nearest neighbor i,j. The long-range Coulomb interaction V_{ij}, written in the Fourier space, has the expression[34]

$$V(\mathbf{q})=\frac{V_C}{2\sqrt{A(q_x,q_y)^2-1}}, \tag{17}$$

with $A(q_x,q_y)=c[\cos(q_x)+\cos(q_y)-2]-1$. The constant c has been estimated to be around 50. According to Eq. (17) the long-range nature of V implies that $\lim_{\mathbf{q}\to 0}V(\mathbf{q})=\infty$. In equilibrium this infinite large constant is compensated by the lattice due to charge neutrality. For a nonequilibrium value of the density this compensation no longer works. As a consequence, the isothermal compressibility, defined by $\kappa=n^2(\partial\mu/\partial n)$, becomes

$$\kappa=\kappa_0+\frac{V(\mathbf{q}\to 0)}{2}n^2>0, \tag{18}$$

where κ_0 means the compressibility without the Coulomb interaction. Whatever the value of κ_0 is, the total κ is according to Eq. (18) always positive preventing any phase separation.

III. COMMENSURATE AND INCOMMENSURATE FLUX PHASES

The expressions for normal state quantities derived above are valid as long as the doping is not too small, where the normal state is unstable with respect to other phases.[23] In particular, the instability towards bond-order states and flux phases has been investigated as function of the coupling J/t (Refs. 7,27) and the temperature T.[6,28] In these works, the new phases have been assumed to be commensurate with a commensurate modulation vector $\mathbf{Q}_c=(\pi,\pi)$. (We use here the terms ''commensurate'' and ''incommensurate'' with respect to the lattice periodicity and not, as in Refs. 35,36 with respect to the electronic filling.) On the other hand, numerical studies[35,36] as well as a zero temperature slave boson calculation[26] indicated that an incommensurate flux state can be more stable than a commensurate one for a general doping. In this section we study this problem in more detail within our approach, especially, also at finite temperatures.

The generalization of Dyson's equation for the Green's function $g(\mathbf{k},i\omega_n)$ to the nonperiodic case is

$$(i\omega_n+\mu)g(\mathbf{k},\mathbf{q},i\omega_n)-\frac{1}{N_c}\sum_{\mathbf{p}}\Sigma(\mathbf{k},\mathbf{p})g(\mathbf{k}-\mathbf{p},\mathbf{q}-\mathbf{p},i\omega_n) =N_c\delta(\mathbf{q}), \tag{19}$$

where we have defined the Fourier transformation by

$$g(\mathbf{k},\mathbf{q},i\omega_n)=\sum_{i,j} g(i,j,i\omega_n)e^{i\mathbf{k}\cdot(\mathbf{R}_i-\mathbf{R}_j)+i\mathbf{q}\cdot\mathbf{R}_j}. \tag{20}$$

$\mathbf{R}_i$ denotes the lattice vector to the site i. The instability towards an incommensurate state causes finite nontranslational parts in Σ and g, which we write as

$$g(\mathbf{k},\mathbf{q},i\omega_n)=g(\mathbf{k},i\omega_n)N_c\delta(\mathbf{q})+\delta g(\mathbf{k},\mathbf{q},i\omega_n), \tag{21}$$

$$\Sigma(\mathbf{k},\mathbf{q})=\Sigma(\mathbf{k})N_c\delta(\mathbf{q})+\phi(\mathbf{k},\mathbf{q}). \tag{22}$$

In order to study the boundary of the incommensurate phase, it is sufficient to linearize Dyson's equation with respect to the nontranslational parts, yielding

$$\delta g(\mathbf{k},\mathbf{q},i\omega_n)=g_0(\mathbf{k},i\omega_n)\phi(\mathbf{k},\mathbf{q})g_0(\mathbf{k}-\mathbf{q},i\omega_n). \quad (23)$$

From Eq. (8), calculated at large N's, we obtain the relation between ϕ and δg:

$$\phi(\mathbf{k},\mathbf{q})=\frac{1}{N_c}\sum_{\mathbf{p}} B(\mathbf{k},\mathbf{q},\mathbf{p})T\sum_n \delta g(\mathbf{p},\mathbf{q},i\omega_n)e^{i\omega_n 0^+}$$

$$=\frac{1}{N_c}\sum_{\mathbf{p}} B(\mathbf{k},\mathbf{q},\mathbf{p})T\sum_n g_0(\mathbf{p},i\omega_n)$$

$$\times g_0(\mathbf{p}-\mathbf{q},i\omega_n)\phi(\mathbf{p},\mathbf{q}). \quad (24)$$

The kernel $B(\mathbf{k},\mathbf{q},\mathbf{p})$ can be written as a sum of separable kernels:

$$B(\mathbf{k},\mathbf{q},\mathbf{p})=t(\mathbf{k}-\mathbf{q})+t(\mathbf{p})+V(\mathbf{q})-\frac{J(\mathbf{q})}{2}-\frac{J(\mathbf{k}+\mathbf{p})}{2}$$

$$=\sum_{\alpha=1}^{6} F_\alpha(\mathbf{k},\mathbf{q})G_\alpha(\mathbf{p},\mathbf{q}), \quad (25)$$

where

$$\vec{F}(\mathbf{k},\mathbf{q})=[t(\mathbf{k}-\mathbf{q}),1,J\cos(k_x),J\sin(k_x),$$
$$J\cos(k_y),J\sin(k_y)], \quad (26)$$

$$\vec{G}(\mathbf{k},\mathbf{q})=\left[1,t(\mathbf{k})+V(\mathbf{q})-\frac{J(\mathbf{q})}{2},-\cos(k_x),\right.$$
$$\left.-\sin(k_x),-\cos(k_y),-\sin(k_y)\right]. \quad (27)$$

The general linearized solution of the nontranslational self-energy can then be written as

$$\phi(\mathbf{k},\mathbf{q})=\sum_\alpha f_\alpha(\mathbf{q})F_\alpha(\mathbf{k},\mathbf{q}). \quad (28)$$

Inserting Eq. (28) in Eq. (24), we obtain the eigenvalue equation

$$\sum_\beta [\delta_{\alpha\beta}-a_{\alpha\beta}(\mathbf{q})]f_\beta(\mathbf{q})=0, \quad (29)$$

where the matrix elements $a_{\alpha\beta}(\mathbf{q})$ in Eq. (29) are defined by

$$a_{\alpha\beta}(\mathbf{q})=\frac{1}{N_c}\sum_{\mathbf{p}} T\sum_n G_\alpha(\mathbf{p},\mathbf{q})F_\beta(\mathbf{p},\mathbf{q})$$

$$\times g_0(\mathbf{p},i\omega_n)g_0(\mathbf{p}-\mathbf{q},i\omega_n). \quad (30)$$

The boundary of the incommensurate phase is determined by the first onset of a nontrivial solution of the homogeneous system Eq. (29). From a different point of view, such instabilities correspond to divergencies of the charge vertex.[29,37] The particular $\mathbf{q}_c$ where such divergencies occur determines the incommensurability vector.

The undoped case has been studied in detail.[7] Due to the Fermi surface topology, all instabilities occur for a commensurate wave vector, and the ground state can be described as a (π,π) flux phase with flux π per plaquette. In our framework, the flux state is characterized by an order parameter

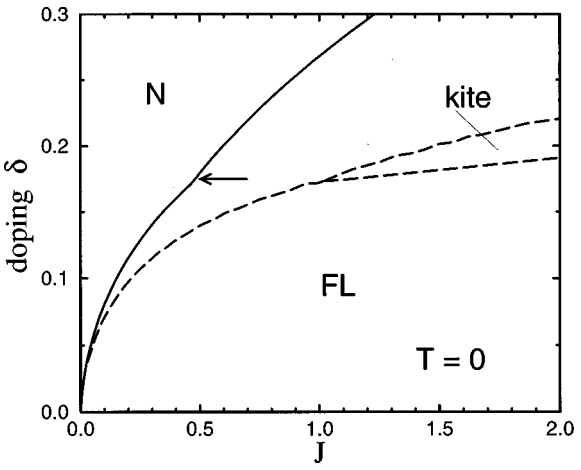

FIG. 1. Solid line: Zero-temperature boundary between normal state N and incommensurate flux state FL. The arrow marks a transition between an incommensurate flux at low and an incommensurate kite phase at high dopings. Dashed lines: Boundaries between normal state N and a commensurate flux or kite state.

Eq. (28) which is imaginary and the antisymmetric combination of its third and fourth component, i.e.,

$$\phi_{\mathrm{FL}}(\mathbf{k},\mathbf{Q}_c)\propto i[\cos(k_x)-\cos(k_y)]. \quad (31)$$

Consequently, a d-wave gap is opened at half-filling of the band. Another state of interest which, however, has a higher energy at $\delta=0$, is the so called ''kite'' phase, which is twofold degenerate and described by the order parameter $\phi_{KI}(\mathbf{k},\mathbf{Q}_c)\propto i[\sin(k_x)\pm\sin(k_y)]$.

It has been argued that for a finite doping both the flux plaquette and the instability or modulation vector $\mathbf{q}_c$ are functions of the doping.[35,36,26] In order to investigate this question in more detail, we have studied instabilities of the normal state with respect to all possible order parameters Eq. (28), which can be constructed from the eigenvectors of the 6×6 matrix in Eq. (29). We found that the instability vector $\mathbf{q}_c$ which can be restricted to the irreducible Brillouin zone corresponding to 1/8 of the total Brillouin zone always lies in the $(0,\pi)$-(π,π) direction, going smoothly to (π,π) for zero doping. Figure 1 shows the calculated phase diagram in the δ-J plane at zero temperature. From now on we put $t=1$ so that all energies such as J are measured in units of t. The dashed lines describe transitions to commensurate states disregarding competing incommensurate states. For $J<1$ there is a transition between the normal state at large dopings to a commensurate flux state at low dopings. For $J>1$ the normal state is with decreasing doping first unstable with respect to the kite phase and the kite phase then with respect to a flux state. Allowing also for incommensurate states the solid line in Fig. 1 shows the boundary of the normal state with respect to an incommensurate flux state at $J<0.5$ and the kite phase at $J>0.5$ where the exact transition point between the two incommensurate states have been marked by an arrow. For $J>0.5$ there is probably another solid line describing a transition between an incommensurate kite and flux phase similar as in the commensurate case. Since we will confine ourselves in the following to the parameter range $J<0.5$ relevant for high-T_c superconductors we have not tried to calculate this additional phase boundary.

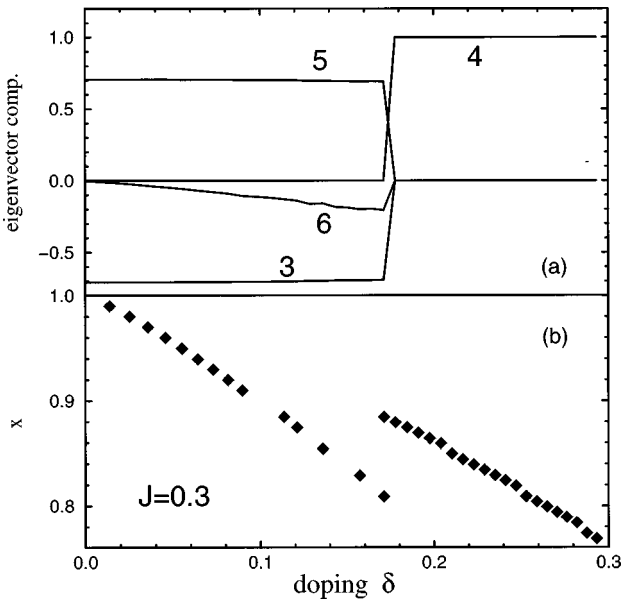

FIG. 2. (a) Evolution of the eigenvector components [3,4,5,6 correspond to $\cos(k_x)$, $\sin(k_x)$, $\cos(k_y)$, $\sin(k_y)$, respectively], along the incommensurate boundary in Fig. 1. (b) Corresponding dependence of the instability vector $\mathbf{q}_c=(1,x)\pi$.

Figure 2(a) characterizes the components of the order parameter along the incommensurate boundary of Fig. 1. The labels 3,4,5,6 correspond to $\alpha=3,4,5,6$ in F_α defined in Eq. (26). For dopings below ~ 0.175 the order parameter is $\phi \sim \cos(k_x)-\cos(k_y)$ and thus has d wave or, using the proper point group classification Γ_3 symmetry. Strictly speaking, ϕ has also a small additional term $\propto \sin(k_y)$ which may occur in incommensurate but not in commensurate states. For dopings above $\delta \sim 0.175$ we have $\phi \propto \sin(k_x)$ and thus an order parameter with Γ_5 symmetry. Writing the instability vector as $\mathbf{q}_c=(1,x)\pi$ the dependence of the value x on the doping is shown in Fig. 2(b). $\mathbf{q}_c$ approaches the commensurate wave vector $\mathbf{Q}_c$ at zero doping. With increasing doping it moves slowly away from $\mathbf{Q}_c$ and exhibits a jump at $\delta \sim 0.175$ where the flux state is replaced by the kite state. For the experimental value $J/t \sim 0.3$ only the flux phase is possible and is the stable phase for dopings below $\delta \sim 0.13$.

Figure 3 shows the phase diagram in the T-δ plane for $J=0.3$. The solid line describes again the incommensurate, the broken line the commensurate state. The inset of that figure shows the temperature dependence of the quantity x of the instability vector $\mathbf{q}_c=(1,x)\pi$. For temperatures larger than ~ 0.014 $\mathbf{q}_c$ coincides with $\mathbf{Q}_c$ so that the broken and solid lines become identical. This behavior is caused by the thermal width of the Fermi function: though the gap in the one-particle density opens not exactly at the chemical potential the thermal smearing around the Fermi surface is large enough to lower the free energy by taking advantage of the high density of states corresponding to the half-filled case. In the following we will assume that the flux state is commensurate. This assumption simplifies considerably calculations which also take superconducting states into account. On the other hand Fig. 3 suggests that this is not an unreasonable approximation.

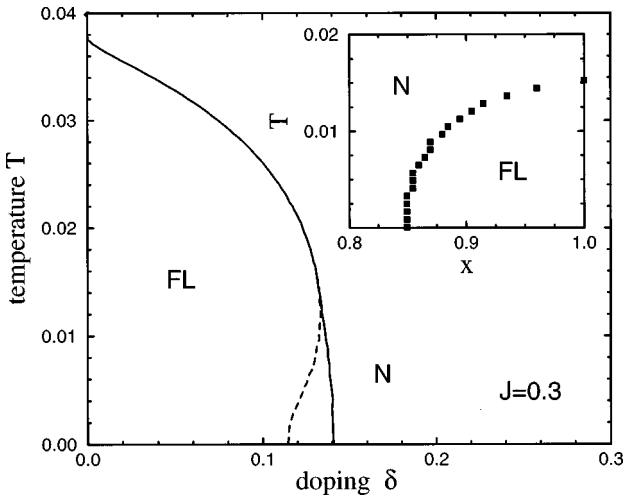

FIG. 3. Incommensurate (solid line) and commensurate (dashed line) phase boundaries in the T-δ plane. Inset: Evolution of the instability vector $\mathbf{q}_c=(1,x)\pi$ as function of T.

IV. COMPETITION BETWEEN SUPERCONDUCTIVITY AND FLUX PHASES

In this section we consider instabilities of the normal and of the flux state with respect to superconductivity. Superconducting instabilities occur at most in $O(1/N)$ of our $1/N$ expansion. This means that it is sufficient to calculate the Green's functions entering the linearized gap equation for superconductivity in the leading order $O(1)$. A detailed study of the normal to superconducting transition showed that the usual mean field term dominated all the other contributions to the kernel of the gap equation. So we will keep just this term and neglect all the other terms which are also of $O(1/N)$. Moreover, it was shown that the leading superconducting instability occurs in the d-wave-like Γ_3 channel so we will consider only a d-wave order parameter. With respect to the order parameter matrix ϕ we will keep the component $\propto \cos(k_x)-\cos(k_y)$ discussed in the last section. The usual charge-density wave order parameter is according to Eq. (28) connected to the columns 1 and 2 and the sum of 3 and 5 and will be included in the next section. Finally, the components $\propto \sin(k_x)$ and $\propto \sin(k_y)$ are associated with the kite phase and do not play a role for $J<0.5$ as shown in the previous section.

In the presence of a commensurate flux phase and singlet superconductivity the operators of the following row vector:

$$\psi(\mathbf{k})=[X^{0\sigma}(\mathbf{k}),X^{\bar{\sigma}0}(-\mathbf{k}),X^{0\sigma}(\mathbf{k}-\mathbf{Q}_c),X^{\bar{\sigma}0}(\mathbf{k}-\mathbf{Q}_c)], \tag{32}$$

are coupled in the Green's functions. We thus define a 4×4 matrix Green's function

$$\hat{G}(k)=-\langle TS\psi^\dagger(k)\psi(k)\rangle/\langle S\rangle, \tag{33}$$

where $\psi^\dagger$ is the hermitian conjugate of ψ, i.e., a column vector. k in Eq. (33) denotes the four-component vector $k=(\mathbf{k},i\omega_n)$. We also note that in the absence of magnetic ground states the Green's functions $\hat{G}$ are spin independent

which allows us to drop all spin indices. Going then over to normalized Green's functions we write the 4×4 matrix $\hat{g}(k)$ as

$$\hat{g}(k)=\begin{pmatrix} g_{11}(k) & g_{12}(k) & g_{13}(k) & 0 \\ g_{21}(k) & g_{22}(k) & 0 & g_{24}(k) \\ g_{13}(k-q_c) & 0 & g_{11}(k-q_c) & g_{12}(k-q_c) \\ 0 & g_{24}(k-q_c) & g_{21}(k-q_c) & g_{22}(k-q_c) \end{pmatrix}. \tag{34}$$

Here we used the fact that the matrix elements $g_{14},g_{23},g_{32},g_{41}$ of $\hat{g}$ must vanish and the explicit expression (32) to connect different matrix elements. We also used the four-component vector $q_c=(\mathbf{Q}_c,0)$. Dyson's equation becomes a 4×4 matrix equation

$$[i\omega_n\hat{I}-\hat{\Sigma}(k)]\hat{g}(k)=\hat{I}. \tag{35}$$

The self-energy matrix $\hat{\Sigma}$ has the general form

$$\hat{\Sigma}(\mathbf{k})=\begin{pmatrix} \Sigma_{11}(\mathbf{k}) & \Delta_{12}(\mathbf{k}) & i\phi_{13}(\mathbf{k}) & 0 \\ \Delta_{21}(\mathbf{k}) & \Sigma_{22}(\mathbf{k}) & 0 & i\phi_{24}(\mathbf{k}) \\ i\phi_{13}(\mathbf{k}-\mathbf{Q}_c) & 0 & \Sigma_{11}(\mathbf{k}-\mathbf{Q}_c) & \Delta_{12}(\mathbf{k}-\mathbf{Q}_c) \\ 0 & i\phi_{24}(\mathbf{k}-\mathbf{Q}_c) & \Delta_{21}(\mathbf{k}-\mathbf{Q}_c) & \Sigma_{22}(\mathbf{k}-\mathbf{Q}_c) \end{pmatrix}. \tag{36}$$

Explicit expressions for the elements of $\hat{\Sigma}$ are obtained from Eq. (8):

$$\Sigma_{ii}(\mathbf{k})=(-1)^{i+1}(1-n)\epsilon_0(\mathbf{k})-\alpha_{ii}(\mathbf{k})+\lambda_{ii}-\mu, \tag{37}$$

with

$$n=\frac{2}{N_c}\sum_{\mathbf{p}} T\sum_n g_{11}(\mathbf{p},i\omega_n)e^{i\omega_n 0^+}, \tag{38}$$

$$\lambda_{ii}=\frac{1}{N_c}\sum_{\mathbf{p}}\left[t(\mathbf{p})-\frac{J(\mathbf{q}=0)}{2}+V(\mathbf{q}\to0)\right] \times T\sum_n g_{ii}(\mathbf{p},i\omega_n)e^{i\omega_n 0^+}, \tag{39}$$

$$\alpha_{ii}(\mathbf{k})=-\frac{1}{2N_c}\sum_{\mathbf{p}} J(\mathbf{k}+\mathbf{p})T\sum_n g_{ii}(\mathbf{p},i\omega_n)e^{i\omega_n 0^+}, \tag{40}$$

and

$$\Delta_{ij}(\mathbf{k})=-\frac{1}{2N_c}\sum_{\mathbf{p}}[J(\mathbf{k}+\mathbf{p})-V_d(\mathbf{k}+\mathbf{p})] \times T\sum_n g_{ij}(\mathbf{p},i\omega_n)e^{i\omega_n 0^+}, \tag{41}$$

$$i\phi_{ij}(\mathbf{k})=-\frac{1}{2N_c}\sum_{\mathbf{p}} J(\mathbf{k}+\mathbf{p})T\sum_n g_{ij}(\mathbf{p},i\omega_n)e^{i\omega_n 0^+}, \tag{42}$$

where $V_d(\mathbf{k})=2V_{nn}[\cos(k_x)+\cos(k_y)]$ is the nearest-neighbor part of the Coulomb interaction. The wave vector $\mathbf{k}$ is either $\mathbf{k}$ or $\mathbf{k}-\mathbf{Q}_c$, so that Eqs. (37)–(42) determine all matrix elements of the self-energy. In particular, all elements of $\hat{\Sigma}$ are independent of frequency in agreement with the notation in Eq. (36). Equations (34) and (36) determine all elements of $\hat{g}$ and $\hat{\Sigma}$. It is easy to see that many of them are actually not independent. Writing for the diagonal elements $\Sigma_{ii}(\mathbf{k})=\epsilon_{ii}(\mathbf{k})+\lambda_{ii}-\mu$ we have $\lambda=\lambda_{ii}$ and

$$\epsilon(\mathbf{k})=\epsilon_{11}(\mathbf{k})=-\epsilon_{22}(\mathbf{k})=-\epsilon_{11}(\mathbf{k}-\mathbf{Q}_c)=\epsilon_{22}(\mathbf{k}-\mathbf{Q}_c). \tag{43}$$

Similarly, one obtains for the elements of the order parameters

$$\Delta(\mathbf{k})=\Delta_{12}(\mathbf{k})=\Delta_{21}(\mathbf{k})=-\Delta_{12}(\mathbf{k}-\mathbf{Q}_c)=-\Delta_{21}(\mathbf{k}-\mathbf{Q}_c), \tag{44}$$

$$\phi(\mathbf{k})=\phi_{13}(\mathbf{k})=\phi_{24}(\mathbf{k})=-\phi_{13}(\mathbf{k}-\mathbf{Q}_c)=-\phi_{24}(\mathbf{k}-\mathbf{Q}_c). \tag{45}$$

In Eq. (44) we have used the fact that Δ can be chosen to be real.

$\hat{\Sigma}(\mathbf{k})$ can easily be diagonalized and one obtains four branches for the excitation spectrum:

$$i\omega_n=\pm E_{\pm}(\mathbf{k})=\pm\sqrt{[\xi(\mathbf{k})\pm(\mu-\lambda)]^2+\Delta(\mathbf{k})^2}, \tag{46}$$

with

$$\xi(\mathbf{k})=\sqrt{\varepsilon(\mathbf{k})^2+\phi(\mathbf{k})^2}. \tag{47}$$

Equation (35) can therefore easily be inverted and the sum over frequencies in Eqs. (38)–(42) carried out. We obtain the following set of self-consistent equations:

$$n=1+\frac{2}{N_c}{\sum_{\mathbf{p}}}',\left\{\frac{\xi(\mathbf{p})-\lambda+\mu}{2E_+(\mathbf{p})}\tanh\left[\frac{E_+(\mathbf{p})}{2T}\right] -\frac{\xi(\mathbf{p})+\lambda-\mu}{2E_-(\mathbf{p})}\tanh\left[\frac{E_-(\mathbf{p})}{2T}\right]\right\}, \tag{48}$$

$$\lambda = \frac{1}{N_c}\sum_{\mathbf{p}}{}' \; t(\mathbf{p})\,\eta(\mathbf{p}) - \frac{1}{2}\left[\frac{J(\mathbf{0})}{2} - V(\mathbf{0})\right]n, \tag{49}$$

$$\alpha(\mathbf{k}) = -\frac{1}{2N_c}\sum_{\mathbf{p}}{}' \; J(\mathbf{k}+\mathbf{p})\,\eta(\mathbf{p}), \tag{50}$$

$$\Delta(\mathbf{k}) = \frac{1}{2N_c}\sum_{\mathbf{p}}{}' \; [J(\mathbf{k}+\mathbf{p}) - V_d(\mathbf{k}+\mathbf{p})]\,\eta_\Delta(\mathbf{p}), \tag{51}$$

$$\phi(\mathbf{k}) = \frac{1}{2N_c}\sum_{\mathbf{p}}{}' \; J(\mathbf{k}+\mathbf{p})\,\eta_\phi(\mathbf{p}), \tag{52}$$

where

$$\eta(\mathbf{k}) = -\frac{\varepsilon(\mathbf{k})}{\xi(\mathbf{k})}\left\{\frac{\xi(\mathbf{k})-\lambda+\mu}{2E_+(\mathbf{k})}\tanh\left[\frac{E_+(\mathbf{k})}{2T}\right] + \frac{\xi(\mathbf{k})+\lambda-\mu}{2E_-(\mathbf{k})}\tanh\left[\frac{E_-(\mathbf{k})}{2T}\right]\right\}, \tag{53}$$

$$\eta_\Delta(\mathbf{k}) = \left\{\frac{\Delta(\mathbf{k})}{2E_+(\mathbf{k})}\tanh\left[\frac{E_+(\mathbf{k})}{2T}\right] + \frac{\Delta(\mathbf{k})}{2E_-(\mathbf{k})}\tanh\left[\frac{E_-(\mathbf{k})}{2T}\right]\right\}, \tag{54}$$

$$\eta_\phi(\mathbf{k}) = \frac{\phi(\mathbf{k})}{\xi(\mathbf{k})}\left\{\frac{\xi(\mathbf{k})-\lambda+\mu}{2E_+(\mathbf{k})}\tanh\left[\frac{E_+(\mathbf{k})}{2T}\right] + \frac{\xi(\mathbf{k})+\lambda-\mu}{2E_-(\mathbf{k})}\tanh\left[\frac{E_-(\mathbf{k})}{2T}\right]\right\}, \tag{55}$$

and the prime on the summation indicates that the sum is restricted to the reduced Brillouin zone.

Equations (48)–(52), together with Eqs. (53)–(55), determine in a self-consistent way all the properties of the system. Moreover, it is possible to construct the thermodynamical potential $\Omega(\mu,T)$ as that function which satisfies the extremal conditions

$$\frac{\delta\Omega}{\delta\alpha(\mathbf{k})} = 0, \quad \frac{\delta\Omega}{\delta\Delta(\mathbf{k})} = 0, \quad \frac{\delta\Omega}{\delta\phi(\mathbf{k})} = 0, \tag{56}$$

together with the conditions $\partial\Omega/\partial\lambda = 0, -\partial\Omega/\partial\mu = n$. Performing a Legendre transformation on Ω one obtains the following expression for the free energy $F(N,T)$:

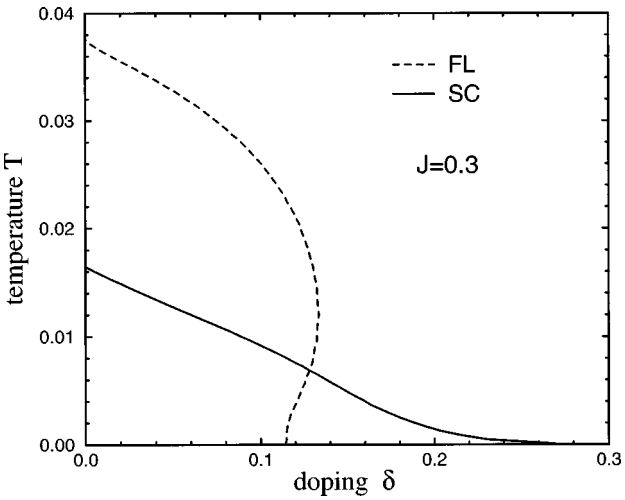

FIG. 4. Phase diagram of the t-J model for decoupled d-wave superconducting (SC) and commensurate flux (FL) order parameters.

$$\begin{aligned} F(N,T) = {} & (\mu-\lambda)(n-1) \\ & - 2T\sum_{\mathbf{k}}{}' \left\{\ln\left[2\cosh\left(\frac{E_+(\mathbf{k})}{2T}\right)\right] + \ln\left[2\cosh\left(\frac{E_-(\mathbf{k})}{2T}\right)\right]\right\} \\ & + \frac{1}{2N_c^2}\sum_{\mathbf{k},\mathbf{p}}{}' \; J(\mathbf{k}+\mathbf{p})\,\eta(\mathbf{k})\,\eta(\mathbf{p}) \\ & + \frac{1}{2N_c^2}\sum_{\mathbf{k},\mathbf{p}}{}' \; J(\mathbf{k}+\mathbf{p})\,\eta_\phi(\mathbf{k})\,\eta_\phi(\mathbf{p}) \\ & + \frac{1}{2N_c^2}\sum_{\mathbf{k},\mathbf{p}}{}' \; [J(\mathbf{k}+\mathbf{p}) - V_d(\mathbf{k}+\mathbf{p})]\,\eta_\Delta(\mathbf{k})\,\eta_\Delta(\mathbf{p}). \end{aligned} \tag{57}$$

After having derived the system of equations for the order parameters we are going to analyze the phase diagram of the t-J model within our approach. We choose the generally accepted value $J = 0.3$ using always t as the energy unit. An estimate of the Coulomb repulsion between nearest neighbor sites V_{nn} may be more controversial. It seems reasonable to assume that V_{nn} is of the same order as J, so we have chosen the value $V_{nn} = 0.5J$. This particular choice means that the contribution from density-density interactions in the J and V_{nn} terms cancel each other in the d-wave superconducting channel, so that superconductivity is driven only by spin-exchange.[24] The role played by V_{nn} and the Coulomb interaction in the phase diagram will be discussed in more detail in the next section.

Figure 4 shows the instability line of the normal state with respect to d-wave superconductivity (solid line) and commensurate flux phase (dashed line) in the T-δ plane assuming that the two phases are uncoupled. T_c of the uncoupled superconducting phase increases with decreasing doping δ.

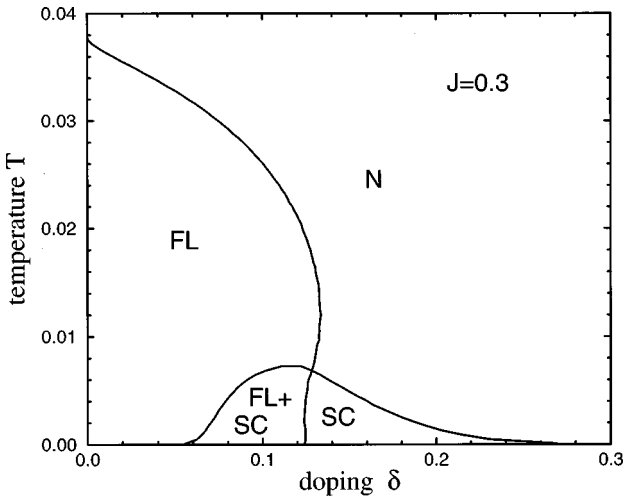

FIG. 5. Phase diagram of the t-J model taking into account the competition between superconductivity and commensurate flux phase.

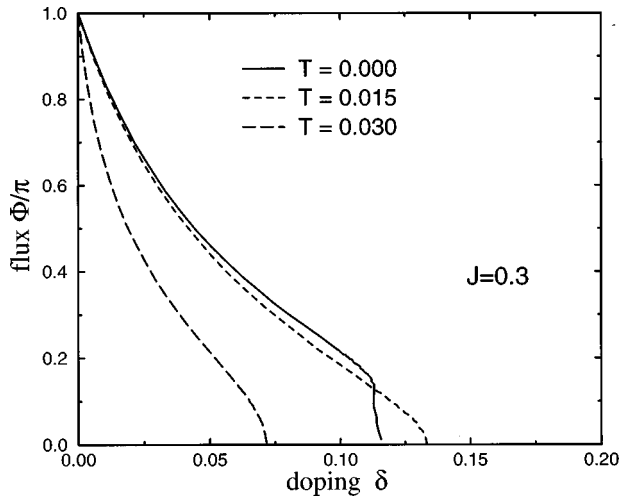

FIG. 6. The flux Φ per plaquette as a function of doping for different temperatures.

This behavior is caused mainly by an increase of the density of states with decreasing δ due to the narrowing of the band and the decreasing distance of the Fermi energy from the Van Hove singularity at the middle of the band. The transition temperature T_{FL} to the flux phase becomes nonzero at around $\delta \sim 0.13$ and assumes very rapidly large value towards lower dopings. Though this instability is caused by nesting properties of the quasi-two-dimensional Fermi surface the dashed line in Fig. 4 indicates that it is much stronger than the instability towards superconductivity. Both phases have order parameters of d-wave symmetry, i.e., nodes along the [1,1] direction and maximum absolute values along the [1,0] and [0,1] directions in $\mathbf{k}$ space. Both phases thus try to reconstruct the Fermi surface mainly around the X and Y points creating there a gap in the single-particle excitation spectrum. In the case of superconductivity the gap opens always right at the Fermi energy and moves with doping. In contrast to that the gap of the flux phase is fixed at the middle of the gap due to the assumed commensurability. Nevertheless, there will be a large competition between the two phases for not too large dopings. Figure 4 suggests that the flux phase is able to reconstruct also electronic states further away from the Fermi surface compared to the superconducting phase which affects mainly electronic states close to the Fermi energy.

Figure 5 shows the phase diagram of the t-J model if the interaction between the flux and superconducting phases is taken into account. For $\delta > \sim 0.13$ only the superconducting phase is stable at low temperatures. At around $\delta = 0.13$ the flux phase order parameter becomes nonzero in the superconducting phase and a coexistence region exists of superconductivity and flux phase. Because the two order parameters have the same symmetry and aim to reconstruct the same parts of the Fermi surface the stronger of the two phases tries to suppress the weaker one. Since $T_{\mathrm{FL}} > T_c$ for $\delta < \sim 0.13$ the superconducting phase is rapidly suppressed for decreasing dopings. As a result the solid line in Fig. 4 which increases monotonously with decreasing doping tends rapidly to zero below $\delta \sim 0.13$ due to the interaction with the flux phase. The maximum value for T_c coincides rather accurately with the onset of the flux phase at $T = 0$. Figure 6 shows the flux per plaquette Φ in the interacting case as a function of doping for three different temperatures. The flux always assumes its maximum value of π at zero doping. With increasing doping or with increasing temperature Φ decays rather fast. In the coexistence region of superconductivity and flux phase Φ is small but nonzero.

Both Figs. 3 and 6 show that at low temperatures $T < \sim 0.01$ an incommensurate flux state is more stable than the commensurate one. In an incommensurate flux state the one-particle gap opens, similar to the case of superconductivity right at the Fermi energy. From this one might expect an even larger competition between flux and superconductivity phases and a more rapid quenching of T_c at low dopings than in the case of a commensurate flux phase. We thus arrive in a natural way at some kind of scenario with a quantum critical point. Omitting superconductivity the metallic state at large dopings passes at zero temperature with decreasing doping through a critical point into a nonmetallic flux state characterized by an order parameter with d-wave symmetry and an incommensurate modulation vector. At finite temperatures the long-range order of the flux state is destroyed but there are still regions of small and large fluctuations in the flux order parameter. Allowing also for superconductivity the surroundings of the quantum critical point becomes superconducting with a T_c which has a maximum at the critical point and decays rapidly at larger or smaller dopings. One attractive feature of our phase diagram is the near coincidence of critical point and maximal T_c which is a necessary consequence of the competition of flux and superconducting phases. This coincidence seems to be a generic feature of high-T_c oxides and does not rely in our approach on parameter choices or fine-tuning.

V. COULOMB INTERACTION AND INCOMMENSURATE CHARGE-DENSITY-WAVE

We have seen in Sec. II that macroscopic phase separation is impossible in the presence of long-range Coulomb forces. However, it is known that in such a situation the charge instability at $\mathbf{q} = 0$ corresponding to phase separation is

shifted to a finite $\mathbf{q}$, leading to an incommensurate charge-density-wave state.[38] Commensurate (CDW) (Ref. 13) or incommensurate charge-density-wave states (ICDW) (Refs. 12,34) have been proposed to account for the metal-insulator transition at $T=0$, the quantum critical point, and the pseudogap features at finite temperatures in the underdoped regime of high-T_c oxides. Though we have proposed a different candidate for the insulating state in the previous section the t-J model may exhibit charge separation and ICDW's in addition to the discussed flux phase. Thus the phase digram in Fig. 5 may have to be modified. We therefore study in the following possible CDW instabilities including in the Hamiltonian also the long-range Coulomb interaction $V(\mathbf{q})$ defined in Eq. (17). For this we consider a general ground state characterized in general by nonvanishing order parameters for d-wave superconductivity and a commensurate d-wave flux state. The corresponding Green's function and self-energies form 4×4 matrices as has been discussed in Sec. IV. On top of this ground state we allow for a small ICDW and check whether its amplitude can be nonzero. The procedure is similar to that used in Sec. III for an incommensurate flux state.

We write the Green's function and the self-energy as

$$\hat{g}(\mathbf{k},\mathbf{q},i\omega_n)=\hat{g}(\mathbf{k},i\omega_n)N_c\delta(\mathbf{q})+\delta\hat{g}(\mathbf{k},\mathbf{q},i\omega_n), \quad (58)$$

$$\hat{\Sigma}(\mathbf{k},\mathbf{q})=\hat{\Sigma}(\mathbf{k})N_c\delta(\mathbf{q})+\hat{\phi}_{\mathrm{CDW}}(\mathbf{k},\mathbf{q}). \quad (59)$$

The first term on the right-hand sides of Eqs. (58) and (59) describe the state with superconductivity and commensurate flux phase, both with d-wave symmetry. $\hat{\phi}_{\mathrm{CDW}}$ and $\delta\hat{g}$ are small nontranslational additions to $\hat{\Sigma}$ and $\hat{g}$ due to the ICDW. It is sufficient to linearize Dyson's equation with respect to the nontranslational parts yielding

$$\delta\hat{g}(\mathbf{k},\mathbf{q},i\omega_n)=\hat{g}(\mathbf{k},i\omega_n)\hat{\phi}_{\mathrm{CDW}}(\mathbf{k},\mathbf{q})\hat{g}(\mathbf{k}-\mathbf{q},i\omega_n). \quad (60)$$

Since we are dealing with a CDW instability $\hat{\phi}_{\mathrm{CDW}}(\mathbf{k},\mathbf{q})$ is diagonal in the 4×4 space and can be written as a linear combination of the two 4×4 matrices:

$$\hat{\tau}_3=\begin{pmatrix}\hat{\sigma}_3 & \hat{0}\\ \hat{0} & -\hat{\sigma}_3\end{pmatrix}, \quad (61)$$

$$\hat{\tau}_0=\begin{pmatrix}\hat{\sigma}_3 & \hat{0}\\ \hat{0} & \hat{\sigma}_3\end{pmatrix}, \quad (62)$$

where $\hat{\sigma}_3$ is the usual third Pauli matrix. Explicit calculations of the diagonal elements of the self-energy using Eq. (8) yield, similar as in Eq. (24), the result

$$\begin{aligned}\hat{\phi}_{\mathrm{CDW}}(\mathbf{k},\mathbf{q})=&\hat{\tau}_3 t(\mathbf{k}-\mathbf{q})\frac{1}{N_c}\sum_{\mathbf{p}}{}'\ T\sum_n \mathrm{Tr}[\hat{\tau}_0\cdot\delta\hat{g}(\mathbf{p},\mathbf{q},i\omega_n)]\\ &+\hat{\tau}_0\frac{1}{N_c}\sum_{\mathbf{p}}{}'\ t(\mathbf{p})T\sum_n \mathrm{Tr}[\hat{\tau}_3\cdot\delta\hat{g}(\mathbf{p},\mathbf{q},i\omega_n)]\\ &+\hat{\tau}_0\left(-\frac{J(\mathbf{q})}{2}+V(\mathbf{q})\right)\frac{1}{N_c}\sum_{\mathbf{p}}{}'\ T\\ &\times\sum_n \mathrm{Tr}[\hat{\tau}_3\cdot\delta\hat{g}(\mathbf{p},\mathbf{q},i\omega_n)]\\ &-\hat{\tau}_3\frac{1}{2N_c}\sum_{\mathbf{p}}{}'\ J(\mathbf{k}+\mathbf{p})T\\ &\times\sum_n [\mathrm{Tr}\hat{\tau}_3\cdot\delta\hat{g}(\mathbf{p},\mathbf{q},i\omega_n)]. \end{aligned}\quad (63)$$

Equation (63) can be written in the more compact form

$$\begin{aligned}\hat{\phi}_{\mathrm{CDW}}(\mathbf{k},\mathbf{q})=&\frac{1}{N_c}\sum_{\mathbf{p}}{}'\ T\sum_n\sum_\alpha \hat{F}_\alpha(\mathbf{k},\mathbf{q})\\ &\times\mathrm{Tr}[\hat{G}_\alpha(\mathbf{p},\mathbf{q})\cdot\delta\hat{g}(\mathbf{p},\mathbf{q},,i\omega_n)], \end{aligned}\quad (64)$$

with the abbreviations

$$\hat{F}(\mathbf{k},\mathbf{q})=\left[t(\mathbf{k}-\mathbf{q})\hat{\tau}_3,\hat{\tau}_0,\frac{J(\mathbf{k})}{2}\hat{\tau}_3\right], \quad (65)$$

$$\hat{G}(\mathbf{k},\mathbf{q})=\left[\hat{\tau}_0,t(\mathbf{k})\hat{\tau}_3+\left(V(\mathbf{q})-\frac{J(\mathbf{q})}{2}\right)\hat{\tau}_0,-\frac{t(\mathbf{k})}{4}\hat{\tau}_3\right]. \quad (66)$$

Similar to Sec. III, the solution of the ICDW order parameter can be written as

$$\hat{\phi}_{\mathrm{CDW}}(\mathbf{k},\mathbf{q})=\sum_\alpha f_\alpha(\mathbf{q})\hat{F}_\alpha(\mathbf{k},\mathbf{q}). \quad (67)$$

Using Eq. (60) the expansion coefficients f_α satisfy the following system of three equations:

$$\sum_\beta [\delta_{\alpha\beta}-a_{\alpha\beta}(\mathbf{q})]f_\beta(\mathbf{q})=0, \quad (68)$$

where the matrix elements $a_{\alpha\beta}(\mathbf{q})$ are defined by

$$\begin{aligned}a_{\alpha\beta}(\mathbf{q})=&\frac{1}{N_c}\sum_{\mathbf{p}}{}'\ T\sum_n \mathrm{Tr}[\hat{G}_\alpha(\mathbf{p},\mathbf{q})\cdot\hat{g}_0(\mathbf{p},i\omega_n)\\ &\cdot\hat{F}_\beta(\mathbf{p},\mathbf{q})\cdot\hat{g}_0(\mathbf{p}-\mathbf{q},i\omega_n)]. \end{aligned}\quad (69)$$

As usual the phase boundary is determined by the onset of the first nontrivial solution of the homogeneous system Eq. (68). The particular $\mathbf{q}_c$ where this occurs determines the incommensurability vector of the ICDW.

Taking also ICDW's into account the calculated phase diagram is shown in Fig. 7 using $J=0.3$ and $V_{nn}/J=0.5$. We also used the long-range Coulomb potential Eq. (17) in the calculation. We characterize its strength by its value V_{nn} between nearest-neighbor sites. Fig. 7 should be compared with Fig. 5 where the same parameter values have been used

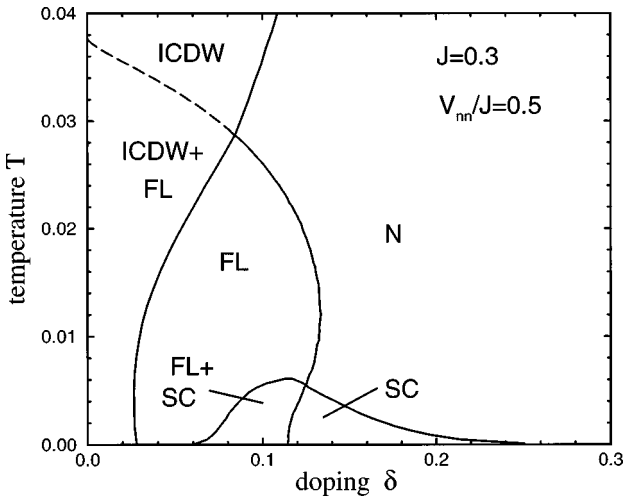

FIG. 7. Phase diagram of the t-J model, considering also an incommensurate charge-density-wave (ICDW). The dashed line between ICDW and ICDW+FL is purely indicative.

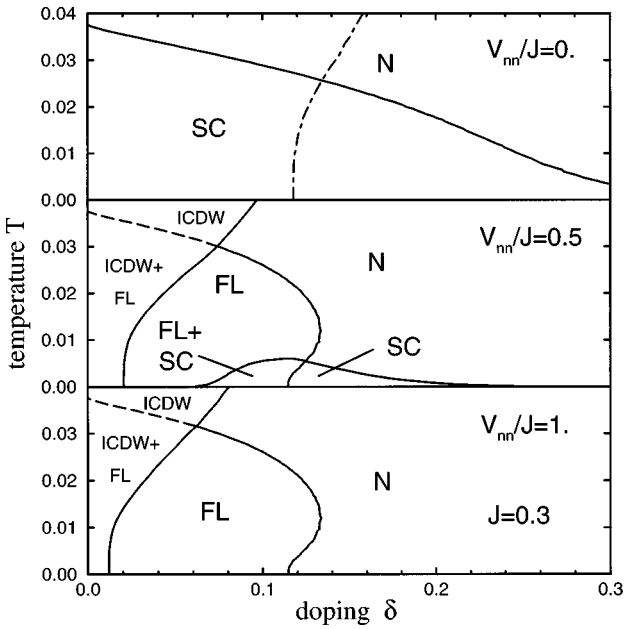

FIG. 8. Evolution of the phase diagram for $J=0.3$ and different Coulomb interaction strengths, characterized by the nearest-neighbor constant V_{nn}. For $V_{nn}=0$ the ICDW instability occurs at $\mathbf{q}_c=0$ corresponding to the divergence of the isothermal compressibility and the onset of phase separation (dot-dashed line).

but the Coulomb interaction was confined to nearest neighbors. The curves for T_c and T_{FL} are very similar in both cases. The region of the flux phase is now, however, split into two regions. In one region at larger dopings only the flux phase is stable; in the other one at lower dopings the flux and the incommensurate charge density phase coexist with each other. At high temperatures the pure ICDW is stable at lower dopings. The figure indicates that the ICDW has no important influence on the T_c curve and, in particular, to its maximum value at optimal doping. The latter is still determined solely by the instability towards the flux phase at around $\delta=0.13$.

Finally we discuss the dependence of the phase diagram on the Coulomb repulsion strength V_C, defined in Eq. (17). Similar to Fig. 7 we use instead of V_C the value V_{nn}, i.e., the Coulomb potential between nearest neighbor sites, to characterize the strength of the Coulomb potential. Changing V_{nn} we can distinguish between two extreme limits. In the case of negligible Coulomb repulsion, i.e., $V_{nn}=0$, the attractive charge-charge term of the t-J model becomes important. As a result the superconducting region becomes large and wipes out the flux phase as shown in the upper panel of Fig. 8. Lowering the temperature from high values one crosses the solid line and enters the superconducting region. The phase boundary between normal and flux phase in Fig. 5 lies now within the superconducting region where according to the calculation this boundary no longer exists. This can be understood from the fact that the superconductivity order parameter has already reconstructed the Fermi surface, especially near the points X and Y, so that an additional order parameter with d-wave symmetry cannot lower further the free energy. At zero temperature the ground state is always superconducting in agreement with the arguments of Ref. 39. Exactly at zero doping the superconducting and the flux phases become equivalent, again in agreement with previous arguments. The isothermal compressibility diverges along the dot-dashed line in the upper panel of Fig. 8. This means that on the left side of this line the normal and superconducting states are unstable as homogeneous phases, and the system separates into two phases, one with zero and the other with a high hole density.

Increasing V_{nn} from zero to finite values the superconducting state is more and more suppressed whereas the boundary to the flux phase is unaffected. This is shown in the middle panel of Fig. 8 for $V_{nn}/J=0.5$ which is the same diagram as Fig. 7. Moreover the superconducting region splits up into a pure superconducting part at larger dopings and a region at lower dopings where the superconducting and the flux order parameters coexist. When V_{nn} exceeds the value J the total effective hole-hole interaction becomes repulsive and superconductivity is totally suppressed. At the same time the instability of the flux phase with respect to an additional ICDW moves towards smaller dopings, i.e., the region of the pure flux phase increases also on the cost of the coexistence region of flux and ICDW phases. This is illustrated in the lower panel in Fig. 8. Figure 8 demonstrates, in particular, two things: with increasing V_{nn} the CDW instabilities move monotonically to lower dopings. The position of these instabilities is in general far away from optimal doping and thus does not influence much the region where superconductivity is the stable phase. For $V_{nn}>0$ optimal doping is more or less determined by the onset of the flux phase at $T=0$ and thus tied to this instability.

We are now in a position to make a comparison of our results with those of other treatments. Reference 33 also enforces the constraint by X operators but does not find any instability of the normal state with respect to a flux phase. Considering the case $N=2$ from the outset Ref. 33 uses a mean-field-like decoupling procedure which violates Luttinger's theorem. For instance, the Fermi surface for $\delta=1/3$ corresponds to half filling in theories where Luttinger's theo-

rem is fulfilled. The absence of a flux phase instability of the normal state as well as a finite T_c for superconductivity even at $J=0$ may be artifacts due this short-coming. Reference 40 calculates the expectation values of bosonic Hubbard operators and the Green's functions with different perturbation expansions finding also solutions for the $n(\mu)$ relation which satisfy Luttinger's theorem. The resulting $T_c(\delta)$ curves are similar to ours but again flux phases and their competition with superconductivity are missing. A basic inconsistency problem inherent in simple decoupling schemes with X operators can also be inferred from a comparison of Ref. 33 with Ref. 40: Calculating expectation values of bosonic Hubbard operators from Green's functions using the projection properties of Hubbard operators or from thermodynamic relations yields different $n(\mu)$ relations. In contrast to that the $1/N$ expansion yields a unique $n(\mu)$ relation and also satisfies Luttinger's theorem. On the other hand we cannot say much about the convergence of the $1/N$ expansion in general. However, in the case of the density fluctuation spectrum it has been shown[37] that the leading order in $1/N$ can already account for most features found in the spectra calculated by exact diagonalizations for $N=2$ for small systems and that the remaining discrepancies nearly vanish if next-to-leading contributions are also taken into account.[41]

Finally we compare our results with treatments where the constraint is enforced using slave particles. One general result of these approaches is[39,22] that the staggered flux phase is always unstable at $T=0$ against d-wave superconductivity. This agrees with our findings, see the upper panel of Fig. 8., Fig. 4 of Ref. 6, and Fig. 1 of Ref. 8, if scaled to our value $J/t=0.3$, show at finite temperatures no or only a very small region at very small dopings where the flux phase is stable. In our case the flux phase is wiped out either by superconductivity or by phase separation as shown in the upper panel of Fig. 8. Taking also Coulomb interactions into account to prevent macroscopic phase separation we find that the flux phase becomes stable above the superconducting phase yielding a maximal T_c of $\delta\sim 0.12$. This value is much larger than the value $\delta\sim 0.03$ obtained in Ref. 8 and also closer to the experimental one of $\delta\sim 0.15$. The decrease of T_c with decreasing δ in the underdoped region is determined in Refs. 6,8 by the condensation temperature of the slave boson particles. Such a Bose condensation does not exist in our approach. Instead the decrease of T_c in the underdoped region is caused in the present approach by the competition of the two d-wave order parameters describing the flux and the superconductivity phase. We also note that experimental data have been interpreted in a phenomenological way as a competition of the superconducting and an unknown phase[15] and the resulting phase diagram is very similar to those of Figs. 5 and 8. The leading order of the $1/N$ expansion is certainly insufficient for a proper description of the undoped case $\delta=0$. It is now generally accepted that the obtained resonance-valence bond instability is in this case somewhat weaker than the instability towards long-range antiferromagnetism. The latter instability, however, can only be obtained by taking higher order contributions of the $1/N$ expansion into account.

VI. CONCLUSIONS

In this paper we have derived the phase diagram of a generalized t-J model taking superconducting, flux, and charge density wave states into account. The investigation was based on the leading expressions of a $1/N$ expansion enforcing the constraints by means of X operators. We found a strong competition between d-wave superconducting and d-wave flux states. As a result the transition temperate T_c for superconductivity showed a maximum near a doping value $\delta=\delta_c\sim 0.13$ for $J/t=0.3$. This value is determined essentially by the onset of an (incommensurate) flux phase at δ_c. To simplify the calculations we assumed the flux phase to be commensurate. We showed that this is correct for $T/t>0.01$. Below this temperature the flux phase is incommensurate which, if taken into account, would presumably not change substantially our conclusions. We also studied the influence of long-range Coulomb forces on the phase diagram. As a result incommensurate charge density waves become stable or coexist with the flux phase at lower dopings well separated from the superconducting region influencing the latter at most in a marginal way.

Our results can be interpreted in terms of a quantum critical point scenario. Disregarding superconductivity the metallic state at large dopings $\delta>\delta_c$ passes to a nonmetallic, incommensurate flux state with d-wave symmetry for $\delta<\delta_c$. Allowing also for superconductivity T_c increases from the overdoped and underdoped sides and shows a maximum around δ_c. On the underdoped side the superconducting phase coexist with the flux phase up to T_c where a pure flux state becomes the most stable state up to the normal state at high temperatures. Two different proposals for the nonmetallic state in the quantum critical point scenario have been made, namely an antiferromagnetic[2] and an incommensurate charge density wave state.[12,34] In comparison with these states we would like to point out three attractive features of our proposal for the nonmetallic state. The instability towards an incommensurate flux phase is a generic feature of the t-J model and is also present if second-nearest-neighbor hopping or Coulomb forces are additionally taken into account. For $J/t<0.5$ the flux phase has d-wave symmetry, i.e., the same symmetry as the most stable superconducting state. Since the flux phase instability is much stronger than the superconducting one T_c is heavily suppressed by the flux phase in the underdoped regime. As a necessary consequence the maximum value for T_c lies near the onset of the flux phase at δ_c.

Finally, we would like to mention that one ingredient of the usual critical point scenario is missing in our treatment due to the approximations adopted by us. Within the critical point scenario it is usually assumed that superconductivity is caused by the singular interaction between quasiparticles mediated by critical fluctuations related to the quantum critical point. The complete $O(1/N)$ contribution to the anomalous self-energy contains, among many other contributions, also a part due to critical fluctuations. This can be seen, for instance, from the divergence of the lowest eigenvalue of the static kernel of the gap equation near the critical doping (see Fig. 1 of Ref. 25). On the other hand, we considered in this paper only the instantaneous contribution in the anomalous self-energy which already determines T_c to a large extent according to Ref. 25. Inclusion of critical fluctuations would presumably enhance T_c somewhat but would not change our results in a serious way.

[1] J. Rossat-Mignod *et al.*, Physica C **185**, 86 (1991).
[2] V. Barzykin and D. Pines, Phys. Rev. B **52**, 13 585 (1995).
[3] P. W. Anderson, Science **235**, 1196 (1987).
[4] I. Affleck, Z. Zou, T. Hsu, and P. W. Anderson, Phys. Rev. B **38**, 745 (1988).
[5] T. Tanamoto, H. Kohno, and H. Fukuyama, J. Phys. Soc. Jpn. **62**, 717 (1993).
[6] M. U. Ubbens and P. A. Lee, Phys. Rev. B **46**, 8434 (1992).
[7] I. Affleck and J. B. Marston, Phys. Rev. B **37**, 3774 (1988).
[8] X. G. Wen and P. A. Lee, Phys. Rev. Lett. **76**, 503 (1996).
[9] P. A. Lee and X. G. Wen, Phys. Rev. Lett. **78**, 4111 (1997).
[10] V. J. Emery and S. A. Kivelson, Physica C **209**, 597 (1993); **235**, 189 (1994).
[11] J. M. Tranquada *et al.*, Phys. Rev. Lett. **78**, 338 (1997).
[12] C. Castellani, C. Di Castro, and M. Grilli, Z. Phys. B **103**, 137 (1997).
[13] R. S. Markiewicz, Phys. Rev. B **56**, 9091 (1997).
[14] J. W. Loram *et al.*, Physica C **235-240**, 134 (1994).
[15] J. R. Cooper and J. W. Loram, J. Phys. I **6**, 2237 (1996).
[16] H. Ding *et al.*, Nature (London) **382**, 51 (1996).
[17] A. G. Loeser *et al.*, Science **273**, 325 (1996).
[18] G. S. Boebinger *et al.*, Phys. Rev. Lett. **77**, 5417 (1996).
[19] F. C. Zhang and T. M. Rice, Phys. Rev. B **37**, 3759 (1988).
[20] G. Kotliar and J. Liu, Phys. Rev. Lett. **61**, 1784 (1988).
[21] A. E. Ruckenstein and S. Schmitt-Rink, Phys. Rev. B **38**, 7188 (1988).
[22] Z. Wang, G. Kotliar, and X. F. Wang, Phys. Rev. B **42**, 8690 (1990).
[23] M. Grilli and G. Kotliar, Phys. Rev. Lett. **64**, 1170 (1990).
[24] A. Greco and R. Zeyher, Europhys. Lett. **35**, 115 (1996).
[25] R. Zeyher and A. Greco, Z. Phys. B **104**, 737 (1997).
[26] D. C. Morse and T. C. Lubensky, Phys. Rev. B **42**, 7994 (1990).
[27] M. Grilli, C. Castellani, and G. Kotliar, Phys. Rev. B **45**, 10 805 (1992).
[28] E. Ercolessi, P. Pieri, and M. Roncaglia, Phys. Lett. A **225**, 331 (1997).
[29] R. Zeyher and M. Kulić, Phys. Rev. B **53**, 2850 (1996).
[30] R. Zeyher, Mol. Phys. Rep. **17**, 247 (1997).
[31] G. Baym and L. Kadanoff, Phys. Rev. **124**, 287 (1961).
[32] M. Kulić and R. Zeyher, Mod. Phys. Lett. B **11**, 333 (1997).
[33] I. S. Sandalov and M. Richter, Phys. Rev. B **50**, 12 855 (1994).
[34] F. Becca, M. Tarquini, M. Grilli, and C. Di Castro, Phys. Rev. B **54**, 12 443 (1996).
[35] P. Lederer, D. Poilblanc, and T. M. Rice, Phys. Rev. Lett. **63**, 1519 (1989).
[36] D. Poilblanc, Y. Hasegawa, and T. M. Rice, Phys. Rev. B **41**, 1949 (1990).
[37] R. Zeyher and M. Kulić, Phys. Rev. B **54**, 8985 (1996).
[38] C. Castellani, C. Di Castro, and M. Grilli, Phys. Rev. Lett. **75**, 4650 (1995).
[39] F. C. Zhang, Phys. Rev. Lett. **64**, 974 (1990).
[40] F. Onufrieva, S. Petit, and Y. Sidis, Phys. Rev. B **54**, 12 464 (1996).
[41] G. Khaliullin and P. Horsch, Phys. Rev. B **54**, 9600 (1996).